NATIONAL ENERGY TECHNOLOGY LABORATORY

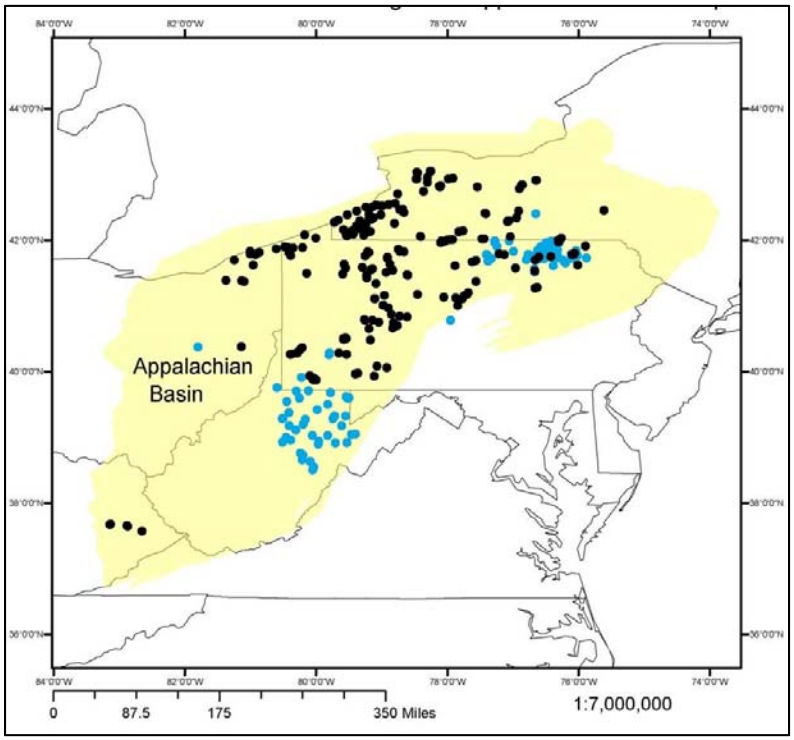

^{2}H, ^{13}C, ^{18}O, ^{226}Ra, and ^{228}Ra Isotope Concentrations in the Appalachian Basin: A Review

28 July 2015

U.S. DEPARTMENT OF ENERGY

Office of Fossil Energy

NETL-TRS-8-2015

Disclaimer

This report was prepared as an account of work sponsored by an agency of the United States Government. Neither the United States Government nor any agency thereof, nor any of their employees, makes any warranty, express or implied, or assumes any legal liability or responsibility for the accuracy, completeness, or usefulness of any information, apparatus, product, or process disclosed, or represents that its use would not infringe privately owned rights. Reference therein to any specific commercial product, process, or service by trade name, trademark, manufacturer, or otherwise does not necessarily constitute or imply its endorsement, recommendation, or favoring by the United States Government or any agency thereof. The views and opinions of authors expressed therein do not necessarily state or reflect those of the United States Government or any agency thereof.

Cover Illustration: This map displays the samples sites for the data discussed in this review. Black sample sites represent oil and gas well data. Blue sample sites represent groundwater data.

Suggested Citation: Mordensky, S.; Schubert, B.; Verba, C.; Hakala, A. *^{2}H, ^{13}C, ^{18}O, ^{226}Ra, and ^{228}Ra Isotope Concentrations in the Appalachian Basin: A Review*; NETL-TRS-8-2015; EPAct Technical Report Series; U.S. Department of Energy, National Energy Technology Laboratory: Albany, OR, 2015; p 32.

An electronic version of this report can be found at:

http://www.netl.doe.gov/research/on-site-research/publications/featured-technical-reports

https://edx.netl.doe.gov/ucr

The data in this report can be accessed from NETL's Energy Data eXchange (EDX) online system (https://edx.netl.doe.gov) using the following link: https://edx.netl.doe.gov/dataset/stable-isotope-data-appalachian-basin

^{2}H, ^{13}C, ^{18}O, ^{226}Ra, and ^{228}Ra Isotope Concentrations in the Appalachian Basin: A Review

Stanley P. Mordensky[1,2], Benjamin Schubert[1,2], Circe Verba[2], Alexandra Hakala[3]

[1] Oak Ridge Institute for Science and Education, MC-100-44, P.O. Box 117, Oak Ridge, TN 37831-0117

[2] U.S. Department of Energy, National Energy Technology Laboratory, 1450 Queen Avenue SW, Albany, OR 97321

[3] U.S. Department of Energy, National Energy Technology Laboratory, 626 Cochrans Mill Road, Pittsburgh, PA 15236

NETL-TRS-8-2015

28 July 2015

NETL Contacts:

Circe Verba, Principal Investigator

Alexandra Hakala, Technical Coordinator

Cynthia Powell, Focus Area Lead

This page intentionally left blank.

Table of Contents

EXECUTIVE SUMMARY **1**
1. INTRODUCTION **2**
2. METHODS **5**
3. OBSERVATIONS **6**
4. CONCLUSION **24**
5. REFERENCES **25**

List of Figures

Figure 1: Appalachian Basin Sample Location 8
Figure 2: Appalachian Basin Groundwater $\delta^{18}O$ H_2O ‰ 9
Figure 3: Appalachian Basin Groundwater $\delta^{2}H$ H_2O ‰ 10
Figure 4: Appalachian Basin Groundwater $\delta^{2}H$ CH_4 ‰ 11
Figure 5: Appalachian Basin Groundwater $\delta^{13}C$ CH_4 ‰ 12
Figure 6: Appalachian Basin Groundwater $\delta^{13}C$ DIC ‰ 13
Figure 7: Appalachian Basin Oil/Gas Well $\delta^{18}O$ H_2O ‰ 14
Figure 8: Appalachian Basin Oil/Gas Well $\delta^{2}H$ H_2O ‰ 15
Figure 9: Appalachian Basin Oil/Gas Well $\delta^{2}H$ CH_4 ‰ 16
Figure 10: Appalachian Basin Oil/Gas Well $\delta^{13}C$ CH_4 ‰ 17
Figure 11: Appalachian Basin Oil/Gas Well $\delta^{13}C$ C_2H_6 ‰ 18
Figure 12: Appalachian Basin Oil/Gas Well $\delta^{13}C$ C_3H_8 ‰ 19
Figure 13: Appalachian Basin Oil/Gas Well $\delta^{13}C$ C_4H_{10} ‰ 20
Figure 14: Appalachian Basin Oil/Gas Well $\delta^{13}C$ DIC ‰ 21
Figure 15: Appalachian Basin Oil/Gas Well ^{226}Ra pCi/L 22
Figure 16: Appalachian Basin Oil/Gas Well ^{228}Ra pCi/L 23

Acronyms, Abbreviations, and Symbols

Term	Description
^{1}H	Stable hydrogen isotope with a mass number of 1
^{2}H	Stable hydrogen isotope with a mass number of 2
^{12}C	Stable carbon isotope with a mass number of 12
^{13}C	Stable carbon isotope with a mass number of 13
^{16}O	Stable oxygen isotope with a mass number of 16
^{18}O	Stable oxygen isotope with a mass number of 18
^{226}Ra	Unstable radium isotope with a mass number of 226
^{228}Ra	Unstable radium isotope with a mass number of 228
C_2H_6	Ethane
C_3H_8	Propane
C_4H_{10}	Butane
CH_4	Methane
CO_2	Carbon dioxide
DIC	Dissolved inorganic carbon
H_2O	Water
IDW	Inverse distance weighting
VSMOW	Vienna Standard Mean Ocean Water

Acknowledgments

This work was completed as part of National Energy Technology Laboratory (NETL) research for the U.S. Department of Energy's (DOE) Complementary Research Program under Section 999 of the Energy Policy Act (EPAct) of 2005. The authors wish to acknowledge Roy Long (NETL Strategic Center for Natural Gas and Oil) and Elena Melchert (DOE Office of Fossil Energy) for programmatic guidance, direction, and support.

The authors extend their appreciation to Dr. Sharma and Dr. Etiope for providing quick replies regarding sample locations and dates; Jennifer Bauer for helping to acquaint the team with ESRI ArcMap; and Kelly Rose, Lucy Romeo, and Jake Nelson for helping debug Python script.

EXECUTIVE SUMMARY

This report focuses on efforts utilized by the U.S. Department of Energy's (DOE) National Energy Technology Laboratory (NETL) which reviews and summarizes 1,141 data points from surface and subsurface isotopes in the Appalachian Basin compiled from publically available datasets. The interpolated, contoured maps show the spatial trends of the isotopes, specifically ^{2}H, ^{13}C, ^{18}O, ^{226}Ra, and ^{228}Ra from. This report reviews groundwater $^{18}O/^{16}O$ and $^{2}H/^{1}H$ concentrations to understand climate factors controlling regional groundwater isotope concentrations, then hydrocarbon $^{2}H/^{1}H$ and $^{13}C/^{12}C$ abundances are reviewed. Thermogenic hydrocarbon material has a different $^{2}H/^{1}H$ and $^{13}C/^{12}C$ signature than biogenic hydrocarbon material. Hence, $^{2}H/^{1}H$ and $^{13}C/^{12}C$ ratios allow inference to the origin of hydrocarbons in natural systems. The groundwater data is primarily focused in West Virginia and southwest and northeast tips of Pennsylvania whereas interestingly, the hydrocarbon well data is focused in the western half of Pennsylvania, Ohio, and New York.

Trend maps shown in this report are based on interpolations using inverse distance weighting, which can help identify the spatial range of isotopic ratios as compared to the Vienna Standard Mean Ocean Water. Furthermore, this report demonstrates that there is a distinct difference in groundwater and hydrocarbon sources that can be applied for various research topics—specifically that of tracing methane related to hydraulic fracturing. Isotopic signatures, in general, aid in identifying methane sources and how they affect groundwater in the Appalachian Basin. Although this collection includes a significant amount of data within the Appalachian Basin, a more accurate representation of the isotopes signatures requires additional data.

1. INTRODUCTION

The Appalachian Basin is a large, northeast-southwest trending depositional basin of Paleozoic stratigraphy. Appalachian Basin units and formations vary in extent throughout the basin (Islas, 2006; Faill, 1997). The deposition of the basin's siliciclastic and carbonate materials began following uplift caused by the Taconic orogeny. Although these differing compositions often comingled, the flux of one composition usually predominated over the other. Interludes of uplift occasionally interrupted deposition, but detritus continued to deposit into the basin until at least the Devonian (Faill, 1997; Swezey, 2002; Islas, 2006). Hydrocarbon-bearing sediments in the basin are between Pennsylvanian and Ordovician in age (Swezey, 2002; Islas, 2006). The Alleghanian Orogeny thrust older metamorphic and igneous rocks toward the west over the younger Paleozoic sedimentary stratigraphy, creating a complex of thrust faults known as the Valley and Ridge Provence that defines much of the eastern margin of the Appalachian Basin. The western Appalachian Basin margin is a mildly sloping, broad homocline that terminates at the Cincinnati Arch (Ryder, 1995).

The Marcellus Shale Formation, found throughout a large extent of the Appalachian Basin, is subject to hydraulic fracturing (fracking) hydrocarbon extraction techniques, which involves the fracturing of rock by a pressurized liquid or gas. Fracturing a rock increases the rock's permeability, which then allows previously isolated pockets of gas to be extracted. Fracking entails pumping large volumes of water and chemicals into the well. The liquid containing fracking chemicals that returns to the surface is known as flowback water. The environmental and public health effects of fracking and produced water management are currently undergoing investigation, however the geological and environmental effects associated with altering subsurface geological structures, pumping chemicals to depth, and potential surface spills of flowback water have not undergone extensive characterization to date.

Observing the isotopic chemistry of a geologic system provides a unique perspective into physical and biological processes that standard chemical measurements do not reflect. Isotopic tracers are an effective way to track fluids from geological formations associated with shale gas production as isotopes are variants of an atom that have the same number of protons but varying numbers of neutrons, which in many cases can be associated with a source geologic material or fluid. Some isotopes are stable; these isotopes do not decay or spontaneously break down into constituent components. The majority of this report discusses stable isotopes (e.g., $^{18}O/^{16}O$ and $^{2}H/^{1}H$) that can be used to track climatological changes across regions and time. After climatological effects are accounted for, $^{2}H/^{1}H$ and $^{13}C/^{12}C$ can provide insight to the origin of a region's hydrocarbon sources such as methane. Other isotopes, such as ^{226}Ra and ^{228}Ra, undergo spontaneous decay, however their presence can suggest the presence of their parent isotopes, which can be used as indicators of fluid sources within a geologic region.

The relative abundances of isotopes fractionate naturally between differing compositions and the gas, liquid, and solid phases of matter. Physical and biological processes sometimes favor one isotope over another. The isotopes, and the factors that control their relative abundances, are described below. Stable isotope ratios are expressed as δ (delta) values in parts per thousand (‰). These values are calculated using isotopic standards specific to each isotope. For example, ^{2}H is expressed as $\delta^{2}H$, which is calculated with the Vienna Standard Mean Ocean Water (VSMOW) Standard and the following equation:

$$\delta\ ^{2}\mathrm{H}\ (\text{in ‰}) = \left[\frac{\left[{}^{2}\mathrm{H}/{}_{1}\mathrm{H}\right]\text{sample}}{\left[{}^{2}\mathrm{H}/{}_{1}\mathrm{H}\right]\text{VSMOW}} - 1\right]1000$$

$\delta^{18}O$ in Groundwater

^{18}O concentrations are largely dependent on changes in the state of water. The heavier ^{18}O fractionates more strongly into lower entropy phases than the lighter ^{16}O. During evaporative processes, ^{18}O becomes enriched in the H_2O fluid and depleted in H_2O vapor. During freezing, ^{18}O preferentially enters solid H_2O. ^{18}O concentrations in the ocean around the tropics and subtropics tend to have higher ^{18}O contents than due to higher evaporation rates. Conversely, oceans in mid-latitude regions, where rain is more abundant, tend to have lower ^{18}O contents (Kendall and Coplen, 2001).

$\delta^{2}H$ in Groundwater

^{2}H, also known as deuterium and often represented by the symbol D, behaves similarly to ^{18}O in hydrological and atmospheric processes and decreases with latitude and altitude. Because the vapor pressure and freezing points of $^{2}H_2O$ are lower than those of H_2O, the concentrations of ^{2}H are higher in the liquid phase than in the vapor, and higher in the solid phase than in the liquid under equilibrium conditions. ^{2}H concentrations are often determined by prevailing temperature and recharge rate. Water bodies with poor outflow and high evaporation, like the Great Salt Lake in Utah, concentrate ^{2}H (Friedman et al., 1964).

$\delta^{2}H$ in Hydrocarbons (CH_4)

Over a regional scale, ^{2}H in CH_4 often reflects the ^{2}H of the regional groundwater, but local processes change isotope concentrations on a smaller scale. Although the ^{2}H of CH_4 does not mirror the ^{2}H of groundwater, it is important to observe regional groundwater ^{2}H when examining ^{2}H-CH_4 data (Kendall and Coplen, 2001). Acetate fermentation depletes ^{2}H and ^{13}C in CH_4 and enriches ^{13}C in CO_2. Methane-oxidizing bacteria preferentially consume lighter CH_4 molecules, enriching the residual ^{2}H and ^{13}C in the CH_4. Thermogenic CH_4 tends to be less depleted (less negative than -175‰) in ^{2}H than biogenic CH_4 (more negative than -175‰). Although biogenic CH_4 is often attributed to shallow aquifer methanogen production, methanogen activity has been recorded in deep substrate (>3,000 m) (Chanton et al., 2005). CH_4 production by deep-living methanogens would result in in a ^{2}H-CH_4 signature that is commonly seen in methane originating from the shallow subsurface. Isotopes in longer hydrocarbon chains (e.g., butane and propane) are less susceptible to changes brought by bacteria processes than CH_4 (Osborn and McIntosh, 2010; Molofsky et al., 2013; Sharma et al., 2013).

$\delta^{13}C$ in Hydrocarbons (CH_4, C_2H_6, C_3H_8, C_4H_{10})

Hydrocarbon ^{13}C is affected by several of the same processes as hydrocarbon ^{2}H. Acetate fermentation and methane-oxidizing bacteria result in depletion and enrichment mechanisms similar to ^{2}H-CH_4. Thermogenic CH_4 tends to be less depleted (less negative than -50‰) in ^{13}C than biogenic CH_4, which appears more depleted (more negative than -50‰). Biogenic CH_4 is often attributed to shallow aquifer methanogen production; however, methanogen activity has been recorded at deep depths (>3,000 m). CH_4 production by deep-living methanogens would

cause a ^{13}C-CH_4 signature to appear to have shallow origins, but in fact, the CH_4 is from a greater depth. Longer hydrocarbon chain isotopes are less susceptible to changes brought by microbiological processes than CH_4 (Osborn and McIntosh, 2010; Molofsky et al., 2013).

$\delta^{13}C$ in Dissolved Inorganic Carbon (DIC)

^{13}C in dissolved inorganic carbon (DIC) varies by soil content. Isotope fractionation between CO_2-HCO_3-$CaCO_3$ results in calcite that is enriched in ^{13}C relative to the CO_2. Marine carbonate rocks usually have a $\delta^{13}C$ close to the Pee Dee Belemnite standard (0 ± 5 ‰). Lacustrine carbonates often have lower $\delta^{13}C$ values due to CO_2 incorporation from decaying plant material. Carbonates that form due to biogenic CH_4 oxidation have negative $\delta^{13}C$ values. Methanogenesis in an organic rich system causes related carbonates to have a very positive $\delta^{13}C$ value (> +20‰) (Kendal, 2014).

^{226}Ra and ^{228}Ra Co-Produced from Oil and Gas Wells

^{226}Ra and ^{228}Ra are radiogenic isotopes with half-lives of 1,600 and 5.75 years, respectively, and are produced through decay from ^{238}U and ^{232}Th, respectively. The presence of Ra in fluid samples indicates the presence of its parent elements (U and Th) in source geologic strata. Radium's decay allows its concentrations to be measured in picocuries (pCi/L), and it is generally found with a 2+ valence. Radium is less soluble than its most common substitution ions (Ba^{2+}, Ca^{2+}, Sr^{2+}); during precipitation, radium becomes enriched in the solid phase and depleted in the solution (Coplen and Huang, 2000).

2. METHODS

Understanding surface and subsurface geochemistry based on an x,y coordinate values may describe geographic trends. The maps in this report were created using ESRI ArcMap 10.1 geostatistical tools. The goal was to interpolate values of cells that lacked sampled points, infer if values are related, and determine if there is a spatial correlation. Different interpolation methods result in different results. Although interpolated surface analyses were completed using two methods, Kriging and Inverse Distance Weighting (IDW), only the IDW interpolations are presented as the Kriging method resulted in more artifacts. The difference in artifact frequency between the two methods is likely a result from how the two interpolation methods treat clustered data differently. Kriging assigns less weight to data in a cluster, whereas IDW does not attempt to account for clustered data. The contours, or isopleths, define a common characteristic and join similar or constant values—in this case stable and unstable isotopes. All stable and unstable isotope data were derived from Coplen and Huang (2000), Coplen and Kendall (2000), Kendall and Coplen (2001), Osborn and McIntosh (2010), Rowan et al. (2011), Risser and Breen (2012), Molofsky et al. (2013), Sharma et al. (2013), Etiope et al. (2013), and Baldassare et al. (2014).

The geographical extent (Figure 1) of the data covers a large section of the Appalachian Basin. This is the amalgamated area of the previous studies, and each one of these individual studies had a different focus depending on the regions and isotopes of interest. Some datasets contain dozens of sample locations over a regional scale. Other datasets consist of only a few locations within a very small area. Some datasets contain multiple values for the same geographical location due to vertical variations when sampling from the subsurface. The Molofsky et al. (2013) data is averaged to a single point as the study does not provide more specific geospatial information for their data. For instances in which a single geographical coordinate contained more than one value, a mean value was used.

Groundwater interpolation analyses were conducted separately from oil and gas well interpolation analyses. Groundwater sample locations are represented with a light blue symbol. To simplify the data displayed on the oil and gas well maps, the data was condensed into three categories based on chronostratigraphy: 1) Cambrian to Base of Marcellus, 2) Marcellus Shale, and 3) Top of Marcellus to Mississippian. The units are represented by red, green, and dark blue symbols, respectively. The contours on the maps containing data from these different layers do not weight one category's values over another. In other words, a contour equally represents all the data that the contour encompasses, regardless of geological age. If there is a large difference in isotope concentrations between two points of the same unit or of different units, different colored contours will run between them.

3. OBSERVATIONS

Appalachian Groundwater Maps

Figure 2: Appalachian Basin $\delta^{18}O$ in Groundwater

$\delta^{18}O$ values become more negative from the west to the east. There are 146 sample locations in this dataset. Data from five sources display the geographical distribution of groundwater $\delta^{18}O$ across the Appalachian Basin (Coplen and Huang, 2000; Coplen and Kendall, 2000; Kendall and Coplen, 2001; Risser and Breen, 2012; Sharma et al., 2013). The Coplen and Huang (2000), Coplen and Kendall (2000), and Kendall and Coplen (2001) data sources are over a decade old, whereas the Risser and Breen (2012) and Sharma et al. (2013) data are much more recently collected.

Figure 3: Appalachian Basin $\delta^{2}H$ in Groundwater

$\delta^{2}H$ values become more negative from the west to the east. There are 142 sample locations in this dataset. Data from five sources display the geographical distribution of groundwater $\delta^{18}O$ across the Appalachian Basin (Coplen and Huang, 2000; Coplen and Kendall, 2000; Kendall and Coplen, 2001; Risser and Breen, 2012; Sharma et al., 2013). The Coplen and Huang (2000), Coplen and Kendall (2000), and Kendall and Coplen (2001) data sources are over a decade old, whereas the Risser and Breen (2012) and Sharma et al. (2013) data are much more recently collected.

Figure 4: Appalachian Basin $\delta^{2}H$ in CH_4 dissolved in Groundwater

$\delta^{2}H$ values are lowest in the northeast and southwest. The Baldassare et al. (2014) data were georeferenced; therefore, there may be small inaccuracies in sample point locations. This dataset is limited in geographic extent. Data from three sources display the geographical distribution of $\delta^{13}C$ in dissolved CH_4 in groundwater (Molofsky et al., 2013; Sharma et al., 2013; Baldassare et al., 2014). The data are clustered in the northeast and southwest regions. The interpolation between these clusters is likely to be inaccurate given the absence of nearby data points. There are 52 sample locations in this dataset.

Figure 5: Appalachian Basin $\delta^{13}C$ in CH_4 dissolved in Groundwater

$\delta^{13}C$ values become more positive traversing southwest to northeast. The Baldassare et al. (2014) data were georeferenced; therefore, there may be small inaccuracies in sample point locations. This dataset is limited in geographic extent. Data from three sources display the geographical distribution of $\delta^{13}C$ in dissolved CH_4 in groundwater (Molofsky et al., 2013; Sharma et al., 2013; Baldassare et al., 2014). The data are clustered in the northeast and southwest regions. The interpolation between these clusters is likely to be inaccurate given the absence of nearby data points. There are 67 sample locations in this dataset.

Figure 6: Appalachian Basin $\delta^{13}C$ in Groundwater DIC

$\delta^{13}C$ values cluster without a regional trend. The clustering of this data into two separate geographic regions without data between these clusters produces artifacts on the interpolated surface. Data from two sources display the geographical distribution of $\delta^{13}C$ in dissolved CH_4 in groundwater (Risser and Breen, 2012; Sharma et al., 2013). There are 62 sample locations in this dataset.

Appalachian Basin Oil/Gas Well Maps

Figure 7: Appalachian Basin $\delta^{18}O$ in Oil/Gas Well H_2O

$\delta^{18}O$ values become more negative from the southeast to the northwest. Areas on the interpolated

surface furthest from data points display artifacts as jagged or abrupt edges. Two sources provide the $\delta^{18}O$ H_2O for this map (Osborn and McIntosh, 2010; Sharma et al., 2013). There are 41 sample locations in this dataset.

Figure 8: Appalachian Basin $\delta^{2}H$ in Oil/Gas Well H_2O

$\delta^{2}H$ values become more negative from the southeast to the northwest. Areas on the interpolated surface farthest from data points display artifacts as jagged or abrupt edges. Two sources provide the $\delta^{2}H$ H_2O for this map (Osborn and McIntosh, 2010; Sharma et al., 2013). There are 41 sample locations in this dataset.

Figure 9: Appalachian Basin $\delta^{2}H$ in Oil/Gas Well CH_4

There is no clear trend in the distribution of $\delta^{2}H$ values, although similar values appear to cluster near each other. Areas of the interpolated surface farthest from sample locations display artifacts. Four sources provide the CH_4 $\delta^{2}H$ data displayed in this map (Osborn and McIntosh, 2010; Molofsky et al., 2013; Sharma et al., 2013; Etiope et al., 2013). There are 92 sample locations in this dataset.

Figure 10: Appalachian Basin $\delta^{13}C$ in Oil/Gas Well CH_4

$\delta^{13}C$ values appear to be lowest around southwestern New York. Areas of the interpolated surface farthest from sample locations display artifacts. Data from four sources provide the $\delta^{13}C$ CH_4 data on this map (Osborn and McIntosh, 2010; Molofsky et al., 2013; Sharma et al., 2013; Etiope et al., 2013). There are 92 sample locations in this dataset.

Figure 11: Appalachian Basin $\delta^{13}C$ in Oil/Gas Well C_2H_6

There is no clear trend in the distribution of $\delta^{13}C$, although similar values appear to cluster near each other. Areas of the interpolated surface farthest from sample locations display artifacts. Three sources provide the $\delta^{13}C$ C_2H_6 data displayed on this map (Osborn and McIntosh, 2010; Molofsky et al., 2013; Etiope et al., 2013). There are 87 sample locations in this dataset.

Figure 12: Appalachian Basin $\delta^{13}C$ in Oil/Gas Well C_3H_8

There is no clear trend in the distribution of $\delta^{13}C$. This dataset is limited in geographic extent. Two sources provide the C_3H_8 $\delta^{13}C$ data displayed on this map (Osborn and McIntosh, 2010; Molofsky et al., 2013). There are eight sample locations in this dataset.

Figure 13: Appalachian Basin $\delta^{13}C$ in Oil/Gas Well C_4H_{10}

$\delta^{13}C$ values increase from the north to the south. This dataset is limited in geographic extent. Osborn and McIntosh (2010) provide the C_4H_{10} $\delta^{13}C$ data displayed on this map. There are six sample locations in this dataset.

Figure 14: Appalachian Basin $\delta^{13}C$ in Oil/Gas Well DIC

$\delta^{13}C$ values increase from north to south, but the correlation is not strong. Two sources provide the $\delta^{13}C$ DIC for this map (Osborn and McIntosh, 2010; Sharma et al., 2013). There are 41 sample locations in this dataset.

Figures 15 and 16: Appalachian Basin ^{226}Ra and ^{228}Ra in Oil/Gas Well

^{226}Ra and ^{228}Ra values appear to behave similarly and display a strong corrleation with geography. Concentrations appear to decrease and then increase moving westward across Pennsylvania. Rowan et al. (2011) provide the data displayed on this map. There are 139 samples in the ^{226}Ra dataset and 127 sample locations in the ^{228}Ra dataset.

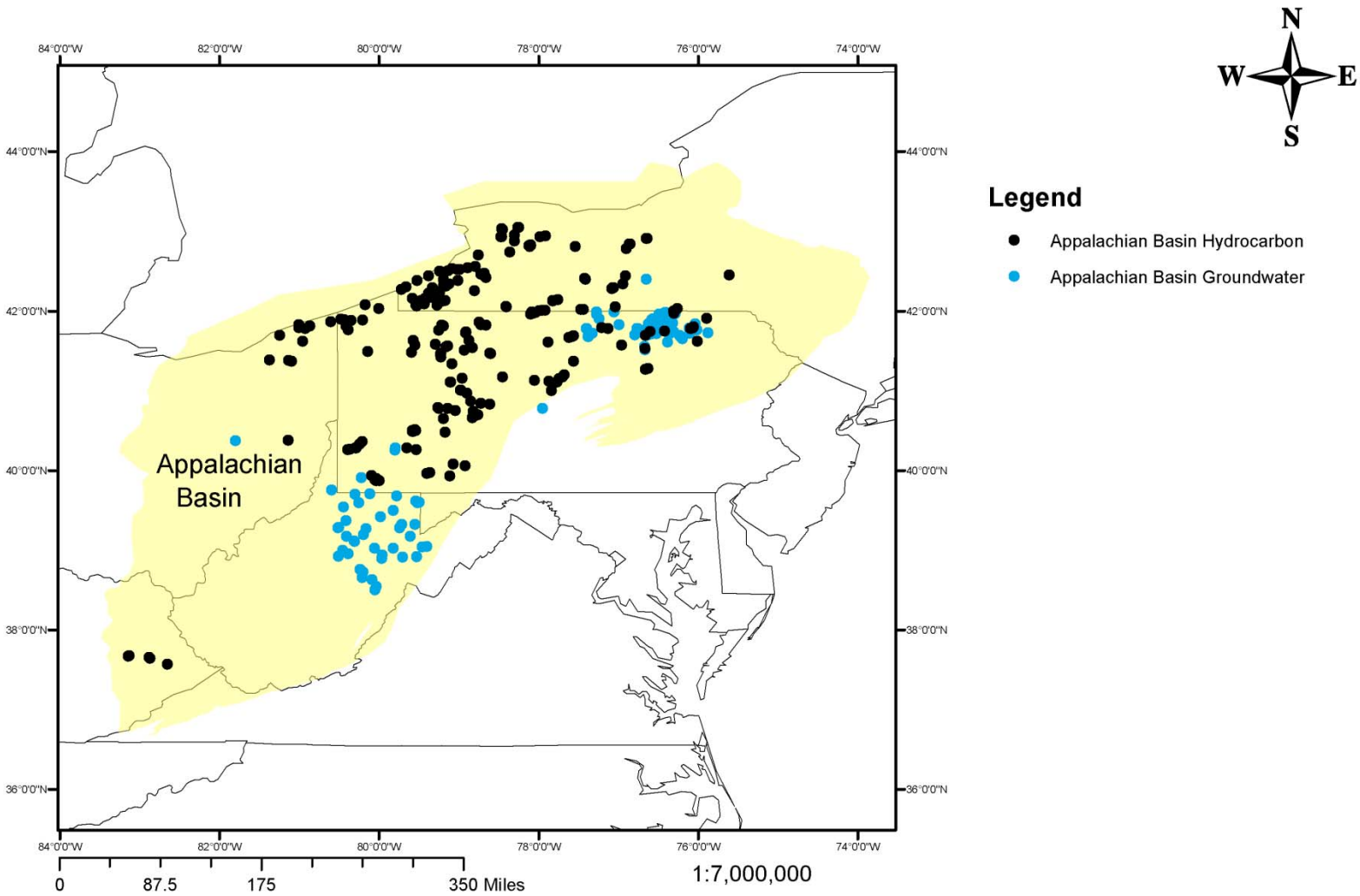

Figure 1: Appalachian Basin Sample Locations

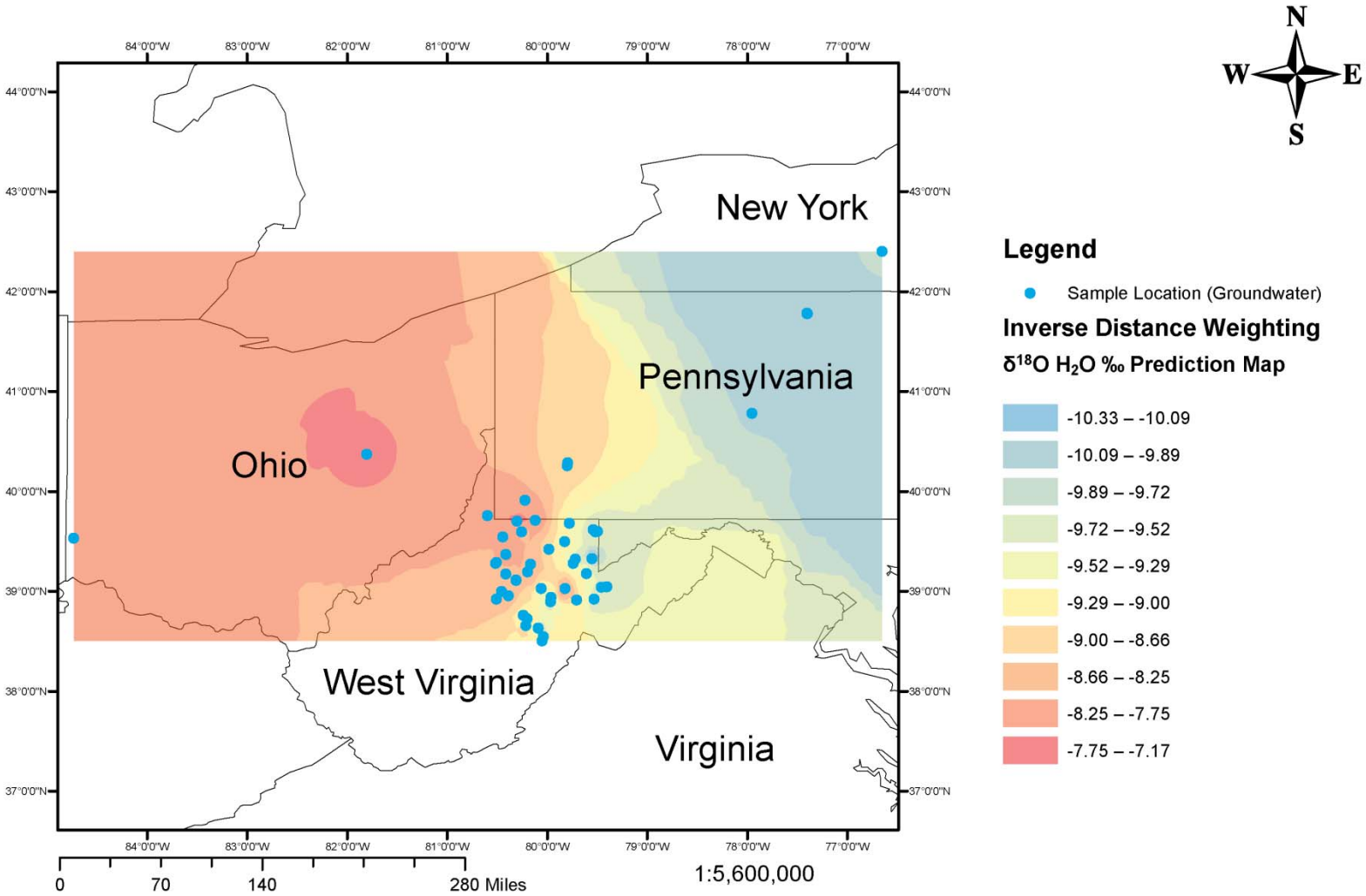

Figure 2: Appalachian Basin Groundwater $\delta^{18}O$ H_2O ‰

This map displays an Inverse Distance Weighted interpolation of Appalachian Basin $\delta^{18}O$ in groundwater. Previous research measured these isotope values from the depicted sample locations (Coplen and Huang, 2000; Coplen and Kendall, 2000; Kendall and Coplen, 2001; Risser and Breen, 2012; Sharma et al., 2013).

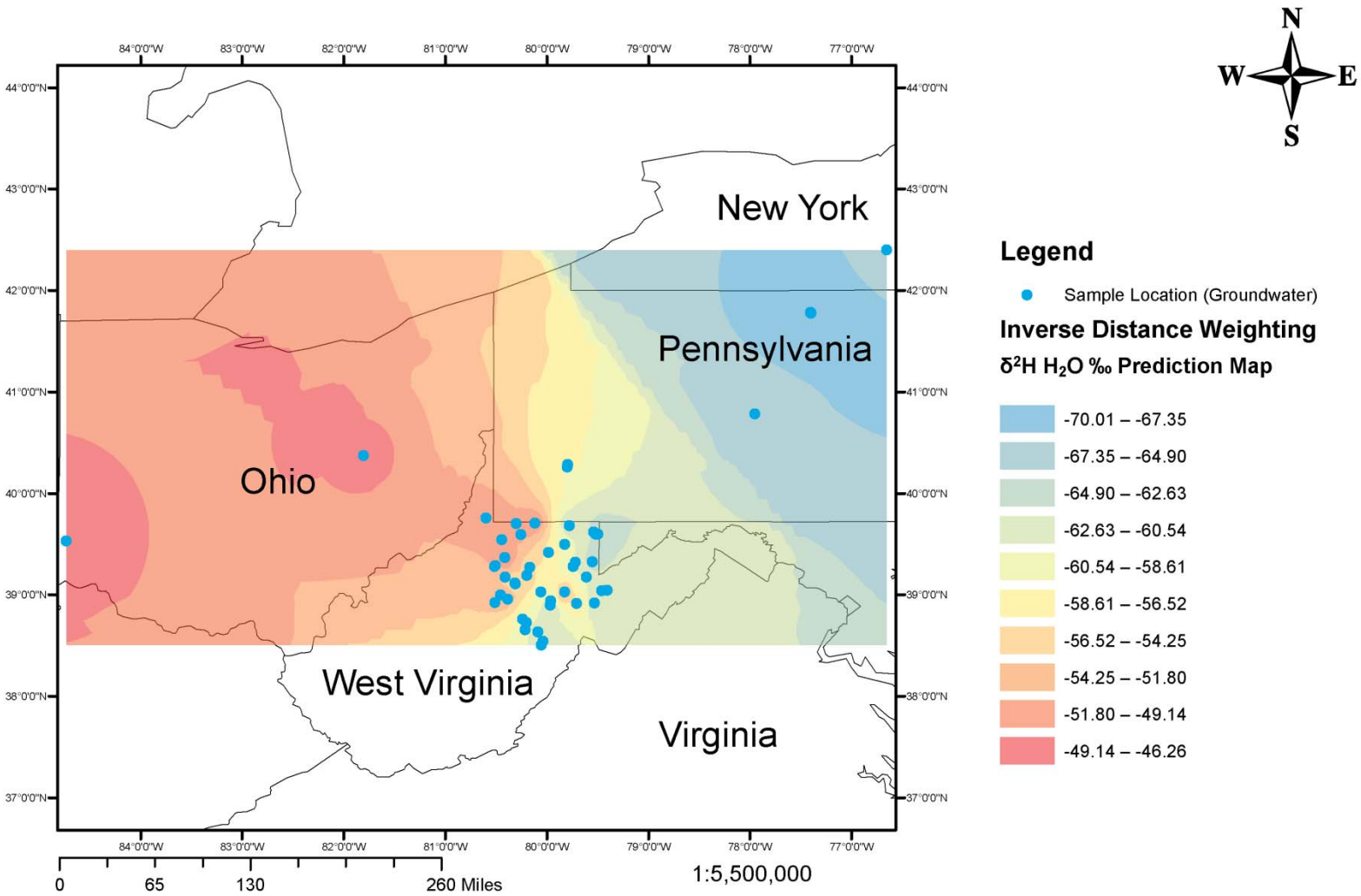

Figure 3: Appalachian Basin Groundwater δ^2H H_2O ‰

This map displays an Inverse Distance Weighted interpolation of Appalachian Basin δ^2H in groundwater. Previous research measured these isotope values from the depicted sample locations (Coplen and Huang, 2000; Coplen and Kendall, 2000; Kendall and Coplen, 2001; Risser and Breen, 2012; Sharma et al., 2013).

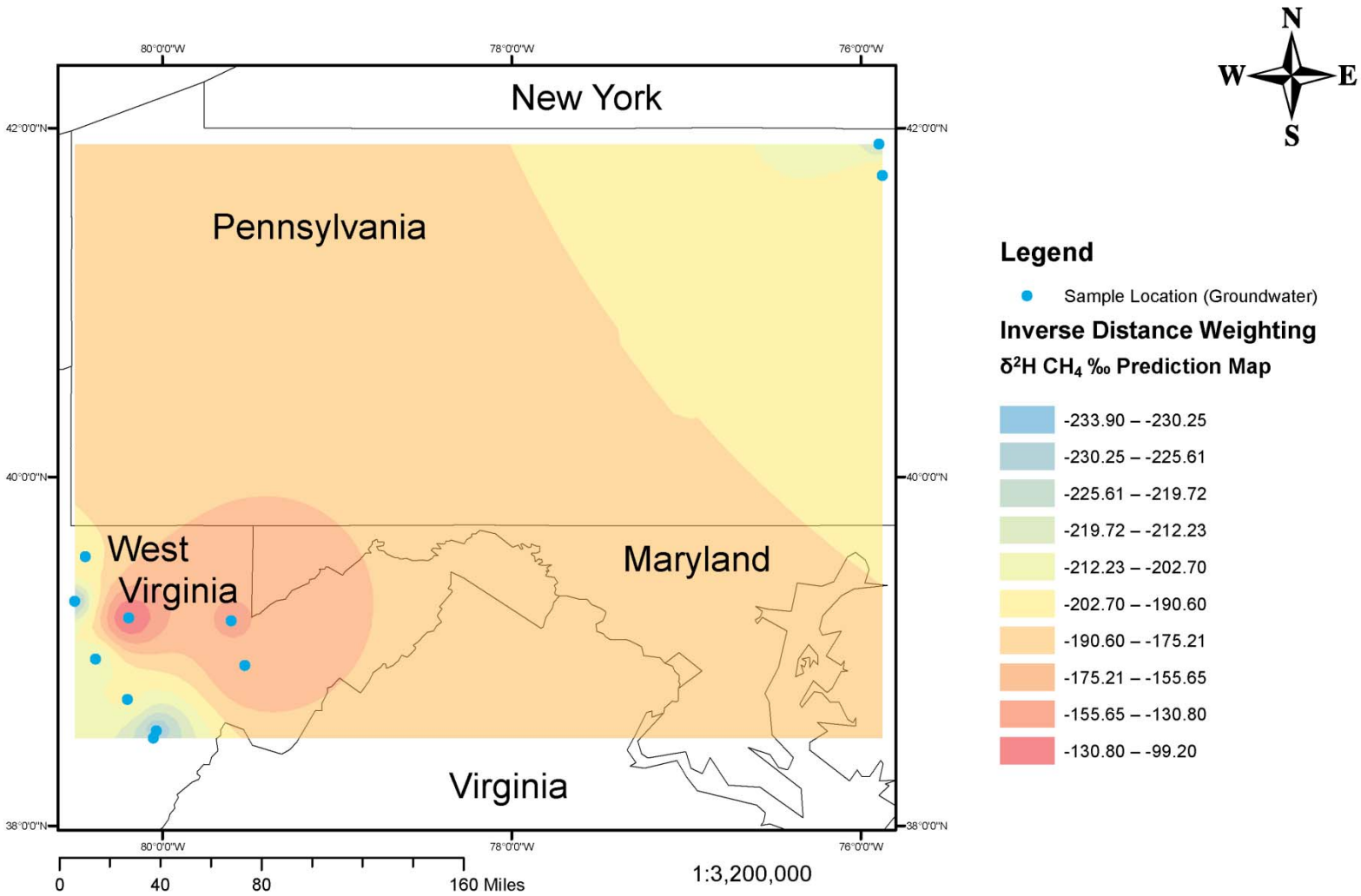

Figure 4: Appalachian Basin Groundwater δ^2H CH_4 ‰

This map displays an Inverse Distance Weighted interpolation of Appalachian Basin δ^2H in CH_4 dissolved in groundwater. Previous research measured these isotope values from the depicted sample locations (Molofsky et al., 2013; Sharma et al., 2013; Baldassare et al., 2014).

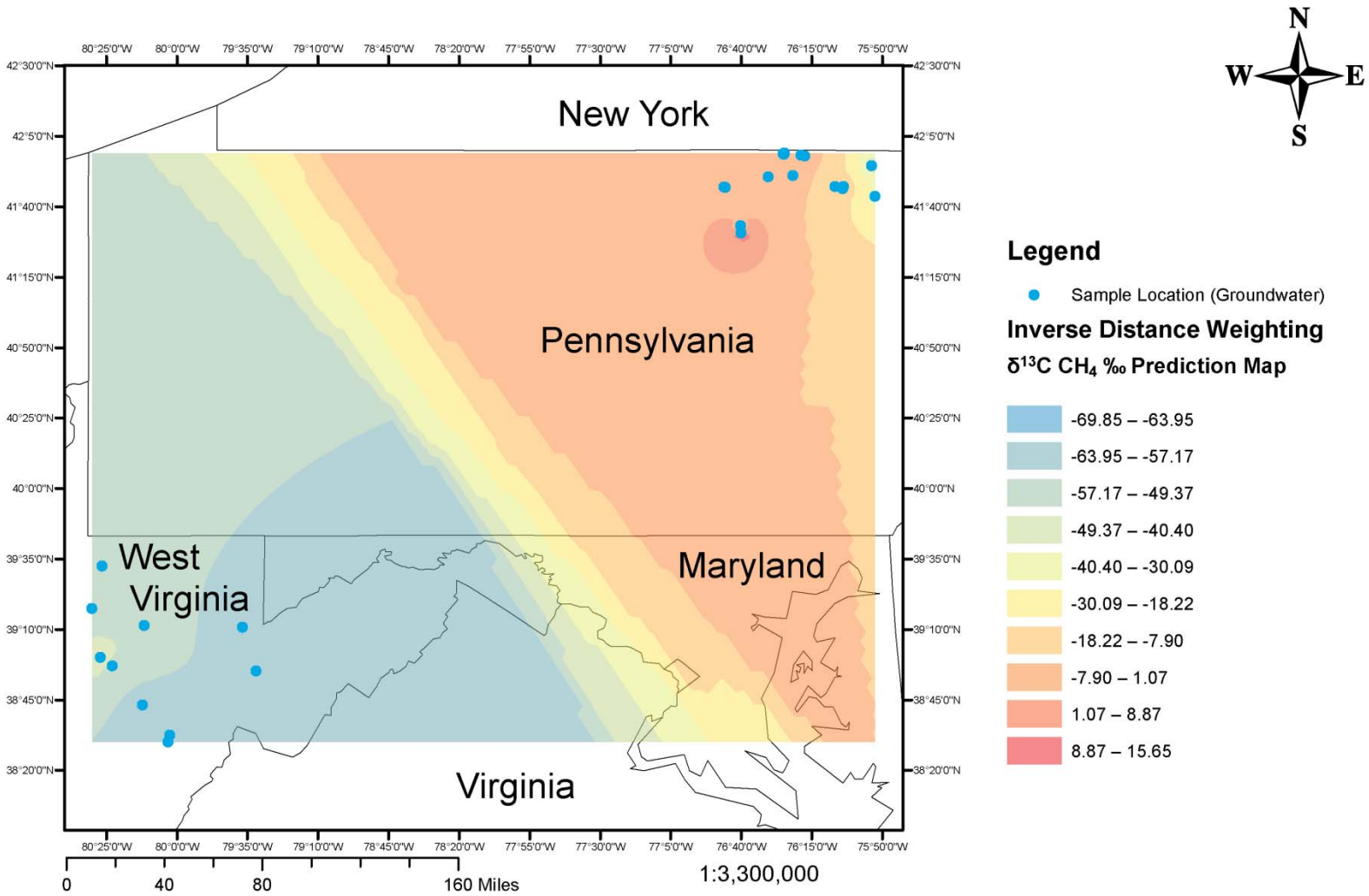

Figure 5: Appalachian Basin Groundwater $\delta^{13}C$ CH_4 ‰

This map displays an Inverse Distance Weighted interpolation of Appalachian Basin $\delta^{13}C$ in CH_4 dissolved in groundwater. Previous research measured these isotope values from the depicted sample locations (Molofsky et al., 2013; Sharma et al., 2013; Baldassare et al., 2014).

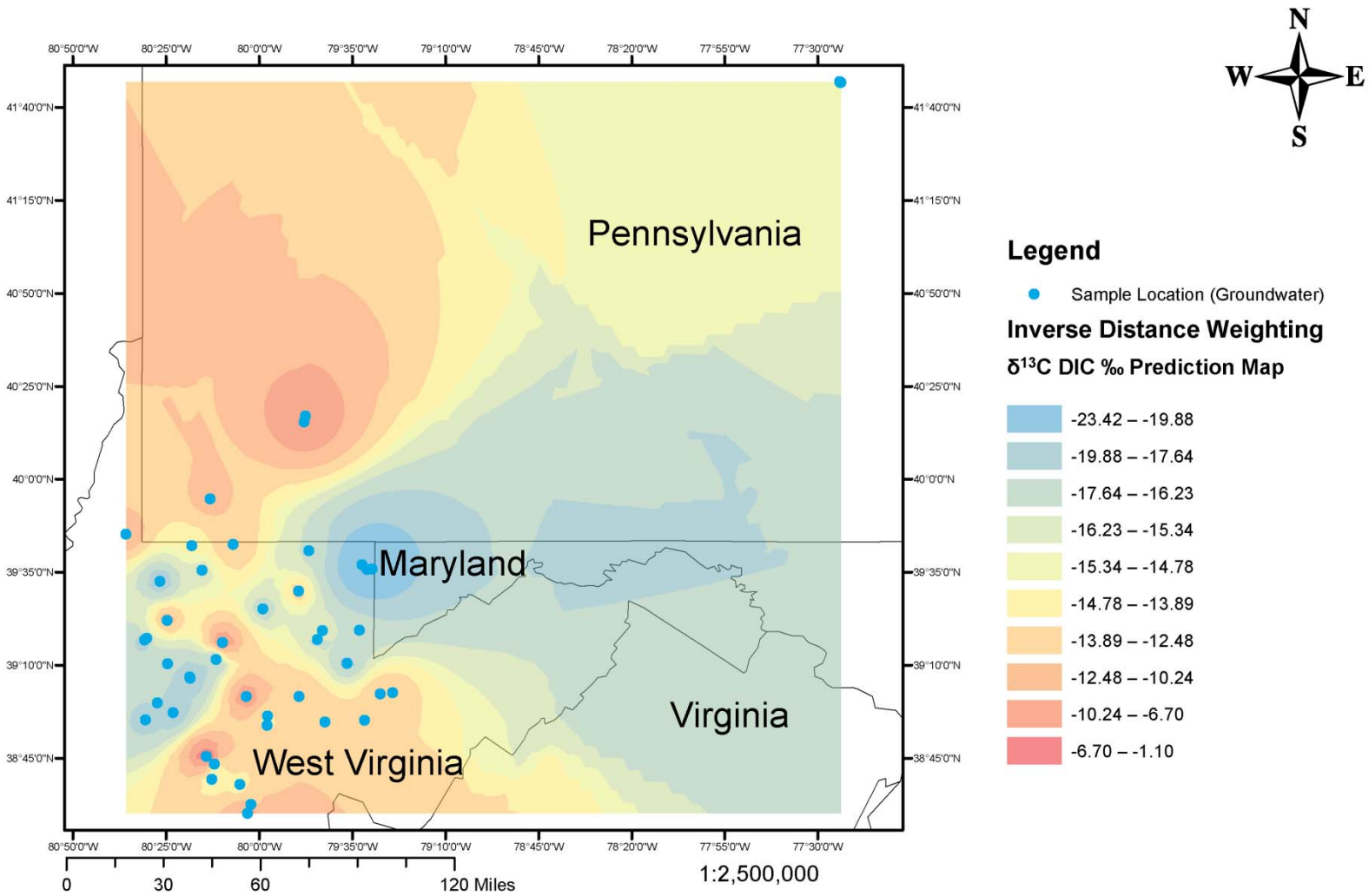

Figure 6: Appalachian Basin Groundwater $\delta^{13}C$ DIC ‰

This map displays an Inverse Distance Weighted interpolation of Appalachian Basin $\delta^{13}C$ in groundwater DIC. Previous research measured these isotope values from the depicted sample locations (Risser and Breen, 2012; Sharma et al., 2013).

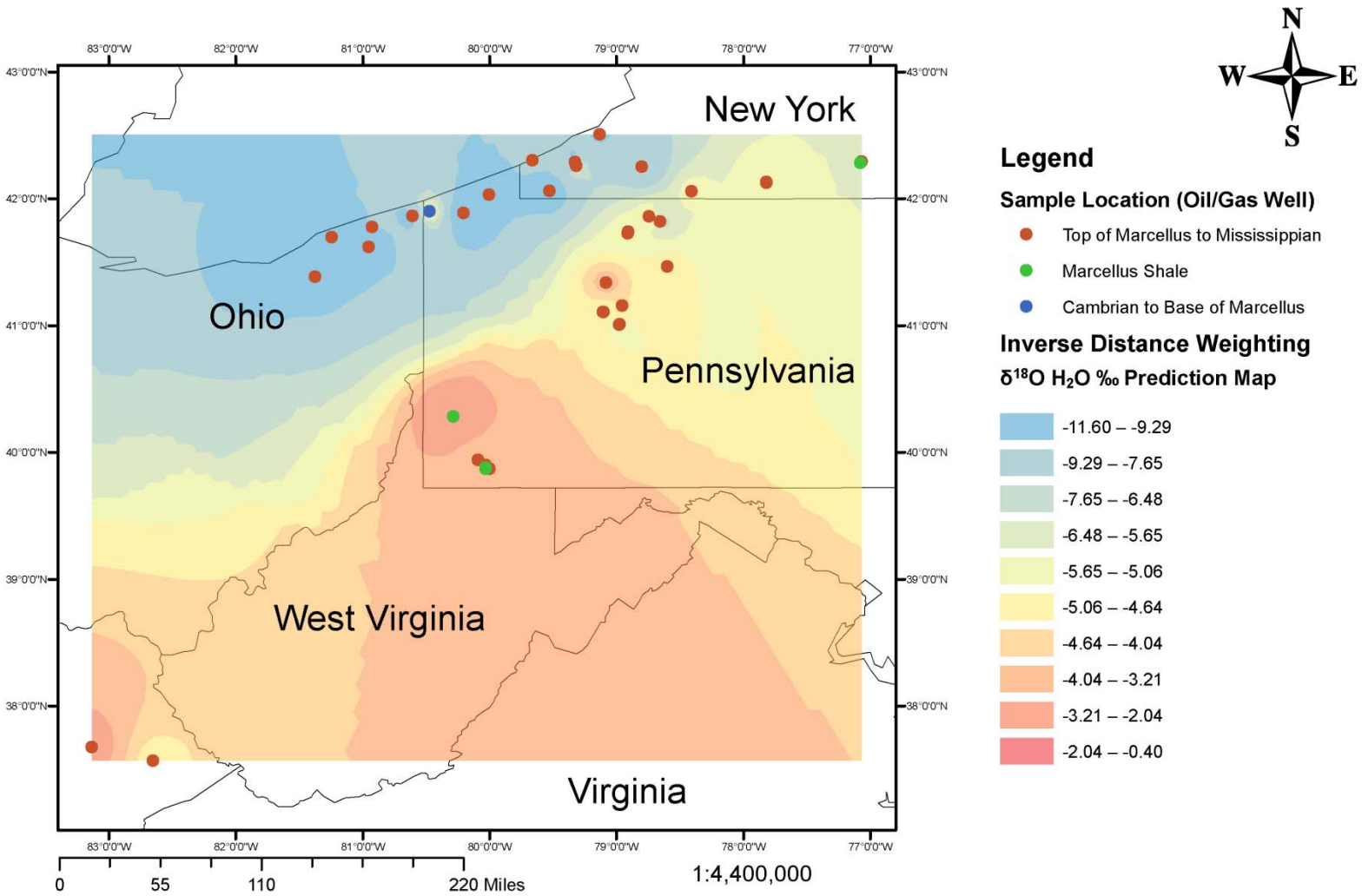

Figure 7: Appalachian Basin Oil/Gas Well $\delta^{18}O$ H_2O ‰

This map displays an Inverse Distance Weighted interpolation of Appalachian Basin $\delta^{18}O$ in H_2O from oil and gas wells. Previous research measured these isotope values from the depicted sample locations (Osborn and McIntosh, 2010; Sharma et al., 2013).

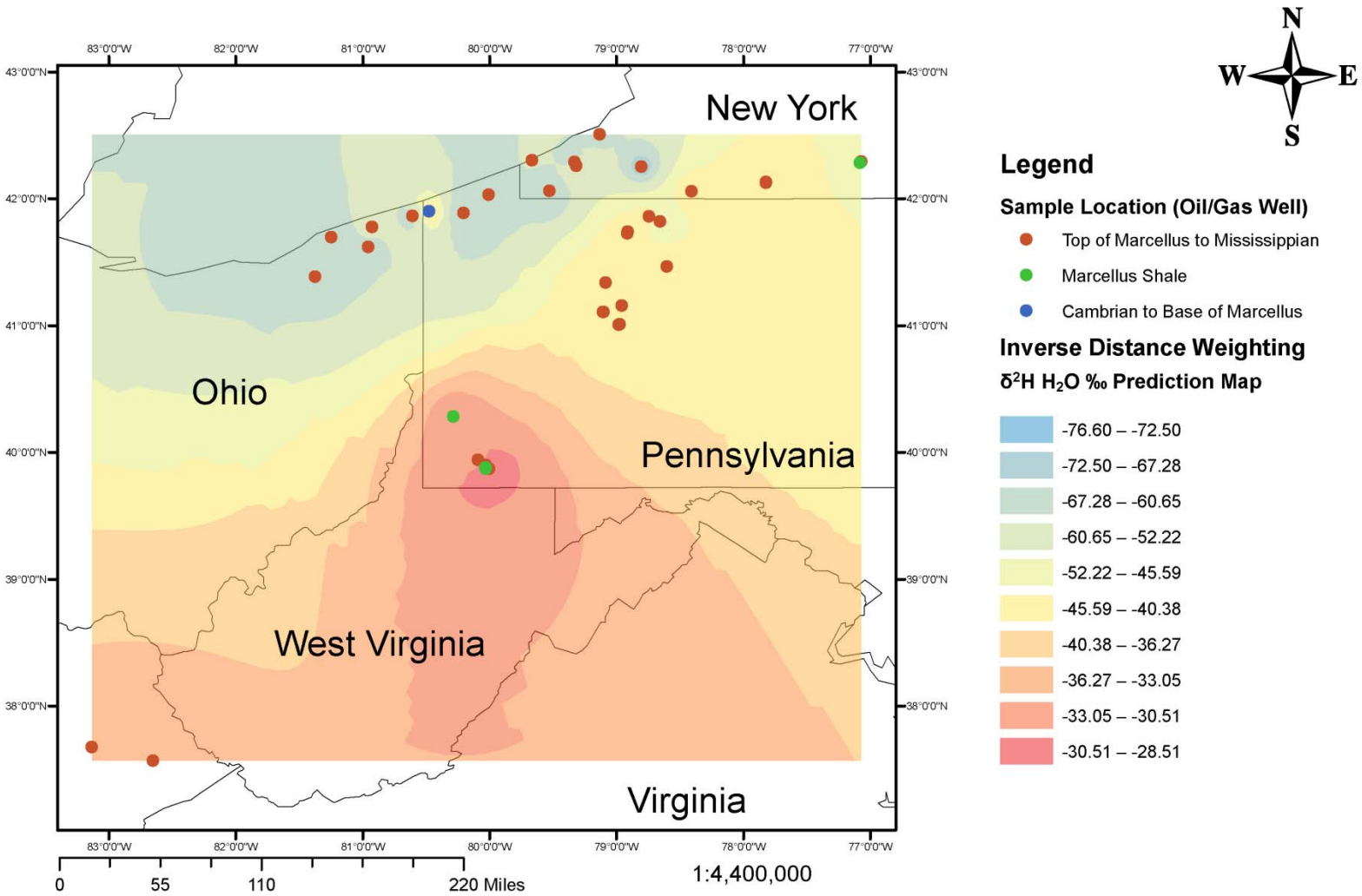

Figure 8: Appalachian Basin Oil/Gas Well δ^2H H_2O ‰

This map displays an Inverse Distance Weighted interpolation of Appalachian Basin δ^2H in H_2O from oil and gas wells. Previous research measured these isotope values from the depicted sample locations (Osborn and McIntosh, 2010; Sharma et al., 2013).

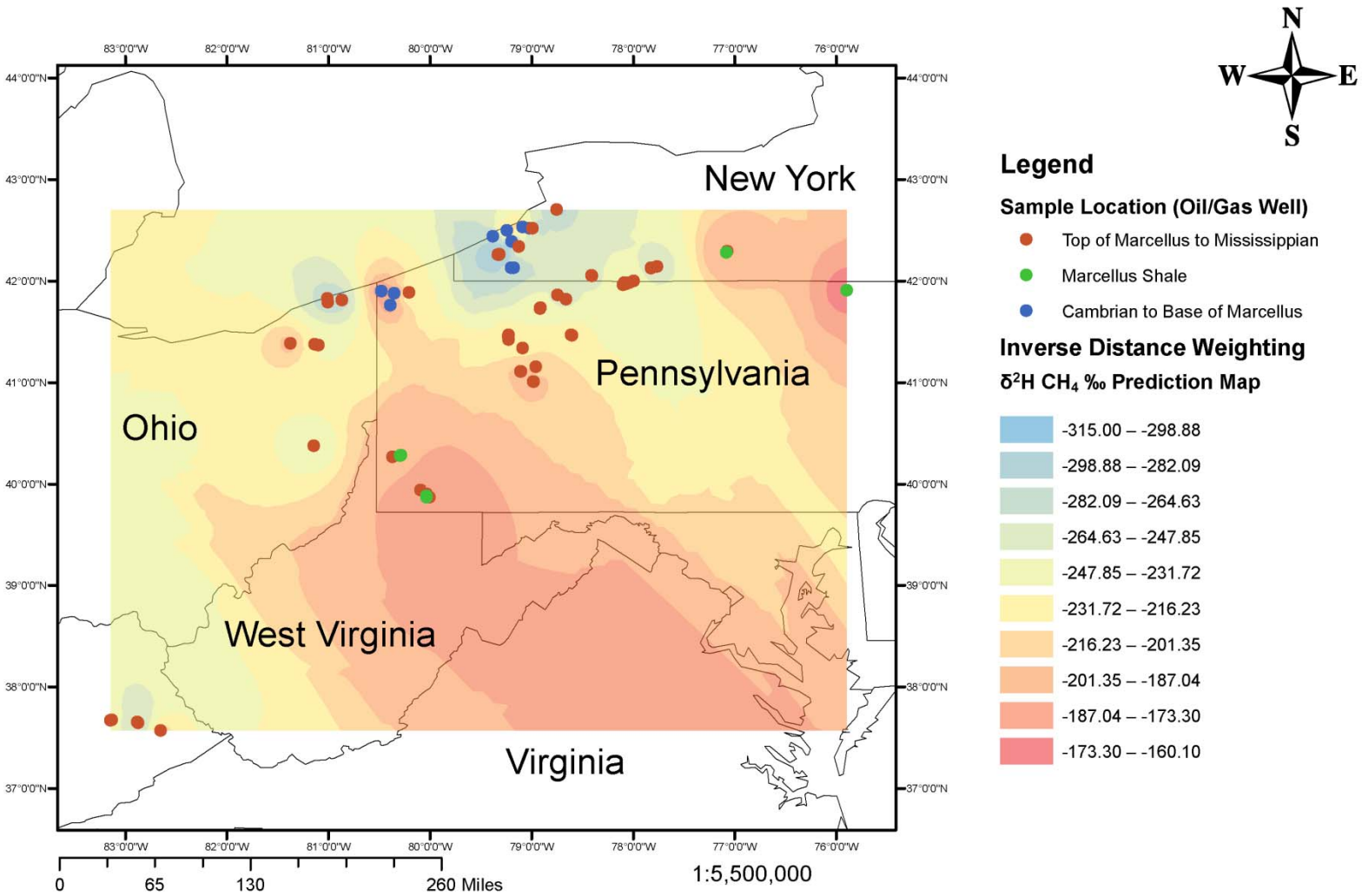

Figure 9: Appalachian Basin Oil/Gas Well δ^2H CH_4 ‰

This map displays an Inverse Distance Weighted interpolation of Appalachian Basin δ^2H in CH_4 from oil and gas wells. Previous research measured these isotope values from the depicted sample locations (Osborn and McIntosh, 2010; Molofsky et al., 2013; Sharma et al., 2013; Etiope et al., 2013).

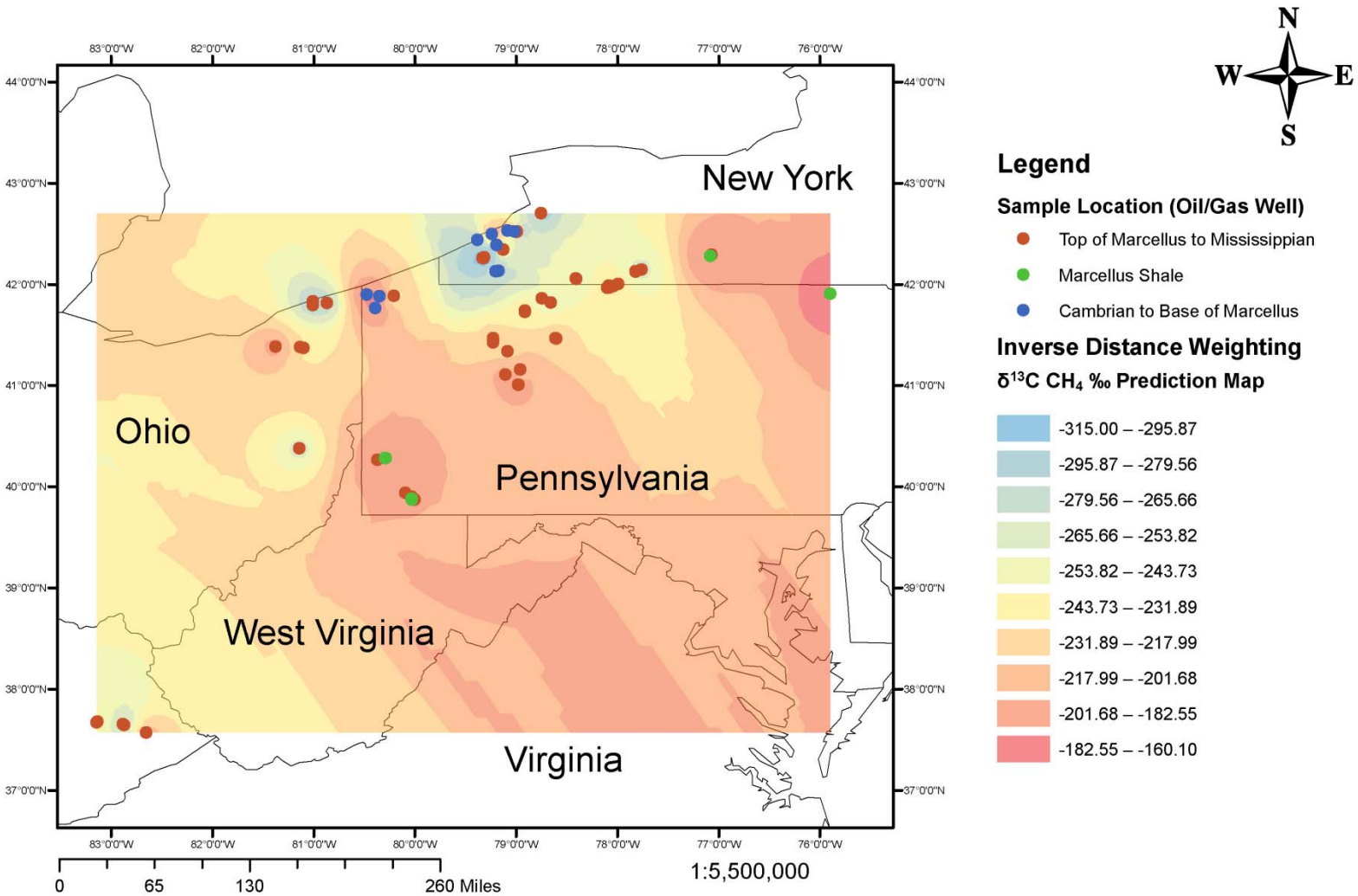

Figure 10: Appalachian Basin Oil/Gas Well $\delta^{13}C$ CH_4 ‰

This map displays an Inverse Distance Weighted interpolation of Appalachian Basin $\delta^{13}C$ in CH_4 from oil and gas wells. Previous research measured these isotope values from the depicted sample locations (Osborn and McIntosh, 2010; Molofsky et al., 2013; Sharma et al., 2013; Etiope et al., 2013).

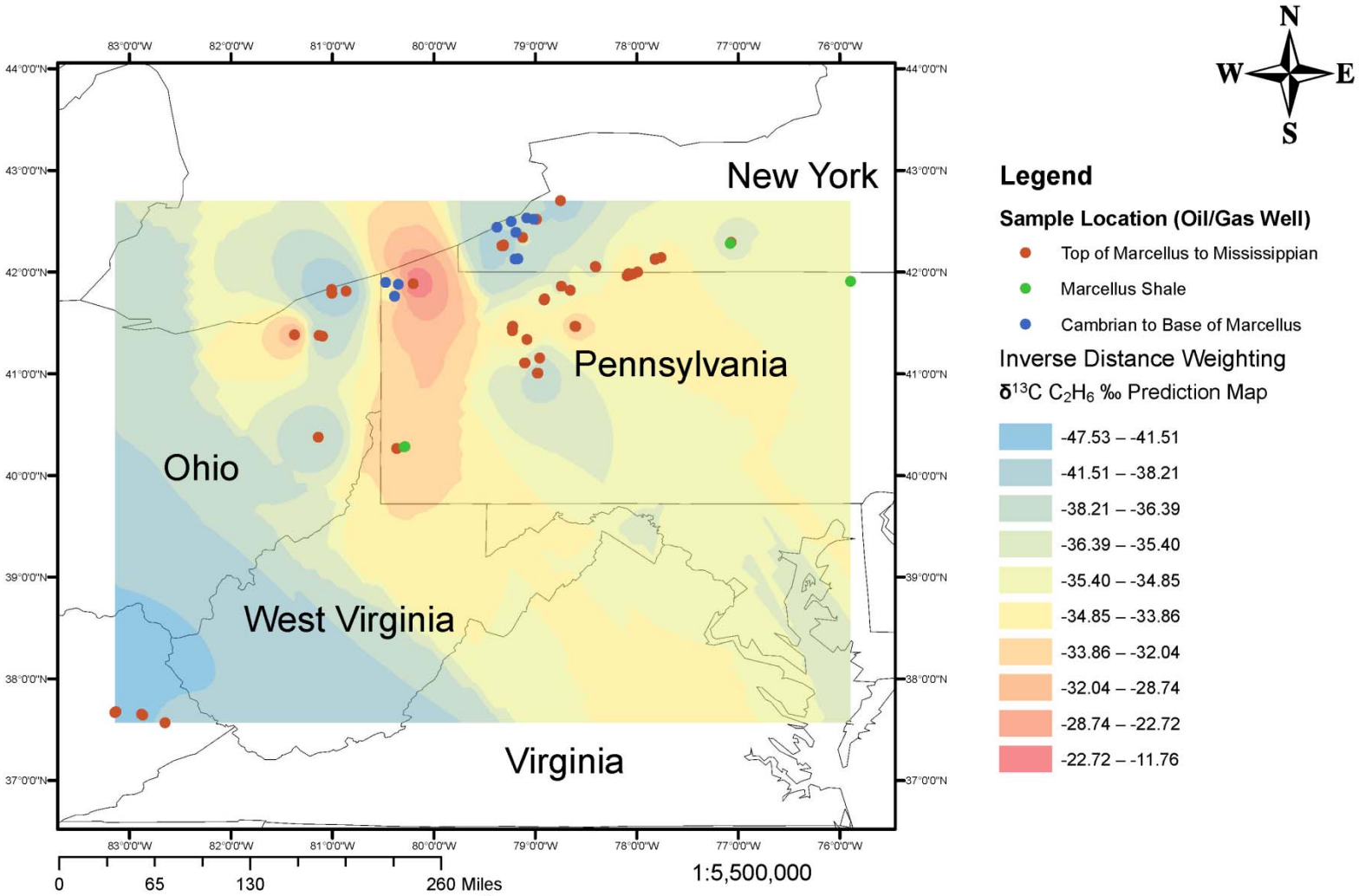

Figure 11: Appalachian Basin Oil/Gas Well $\delta^{13}C$ C_2H_6 ‰

This map displays an Inverse Distance Weighted interpolation of Appalachian Basin $\delta^{13}C$ in C_2H_6 from oil and gas wells. Previous research measured these isotope values from the depicted sample locations (Osborn and McIntosh, 2010; Molofsky et al., 2013; Etiope et al., 2013).

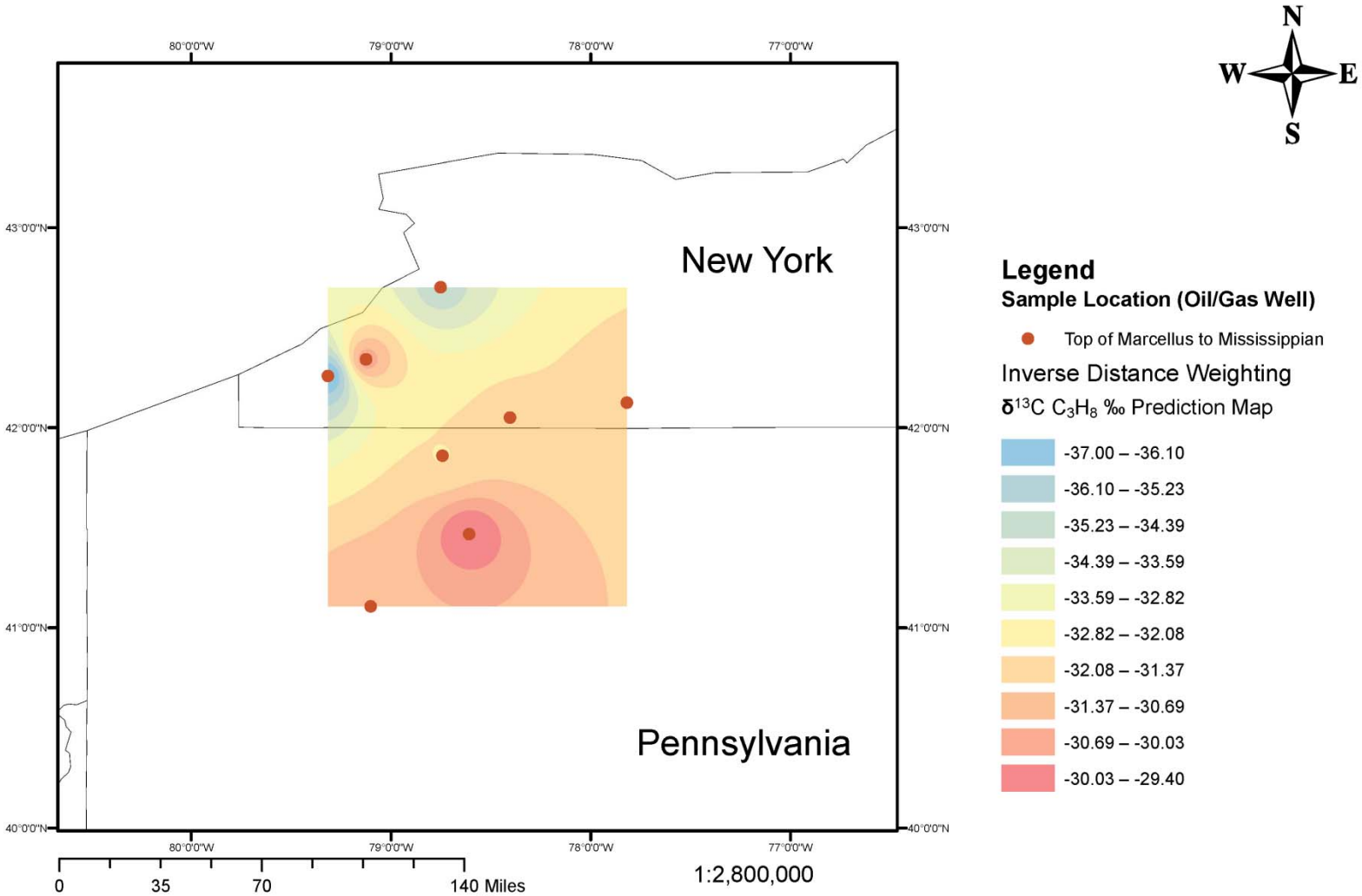

Figure 12: Appalachian Basin Oil/Gas Well $\delta^{13}C$ C_3H_8 ‰

This map displays an Inverse Distance Weighted interpolation of Appalachian Basin $\delta^{13}C$ in C_3H_8 from oil and gas wells. Previous research measured these isotope values from the depicted sample locations (Osborn and McIntosh, 2010; Molofsky et al., 2013).

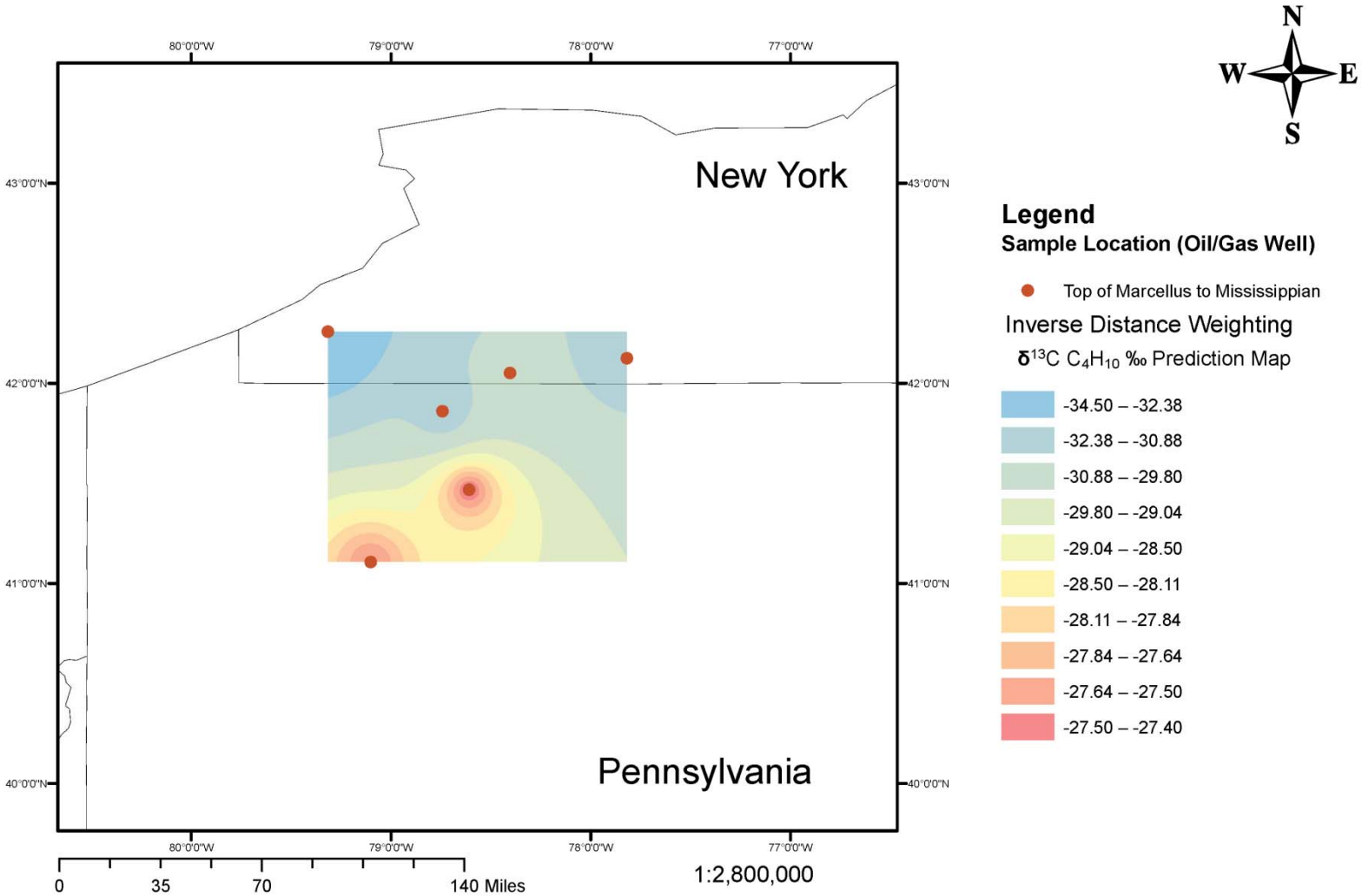

Figure 13: Appalachian Basin Oil/Gas Well $\delta^{13}C$ C_4H_{10} ‰

This map displays an Inverse Distance Weighted interpolation of Appalachian Basin $\delta^{13}C$ in C_4H_{10} from oil and gas wells. Previous research measured these isotope values from the depicted sample locations (Osborn and McIntosh, 2010).

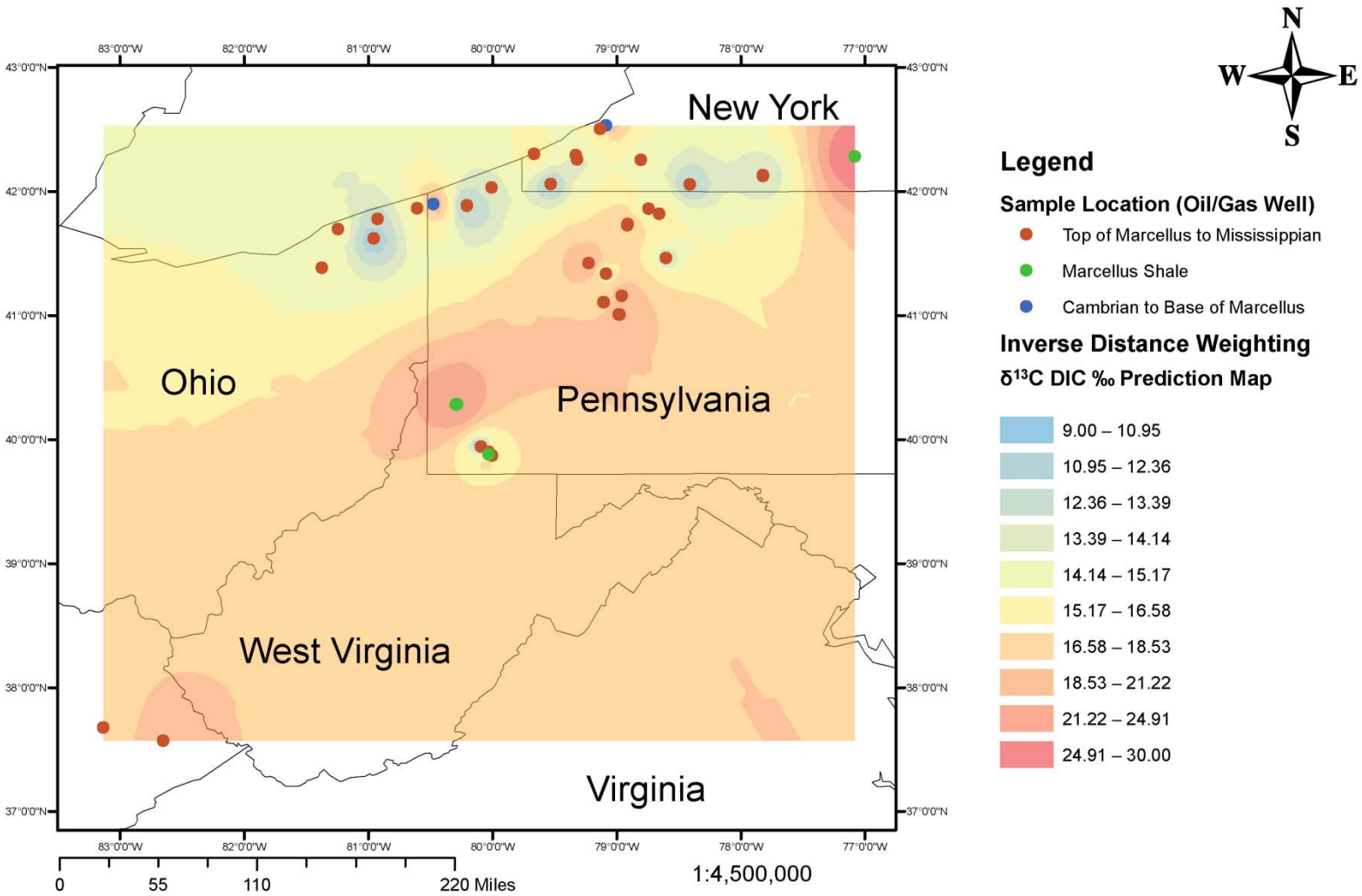

Figure 14: Appalachian Basin Oil/Gas Well $\delta^{13}C$ DIC

This map displays an Inverse Distance Weighted interpolation of Appalachian Basin $\delta^{13}C$ in DIC from oil and gas wells. Previous research measured these isotope values from the depicted sample locations (Osborn and McIntosh, 2010; Sharma et al., 2013).

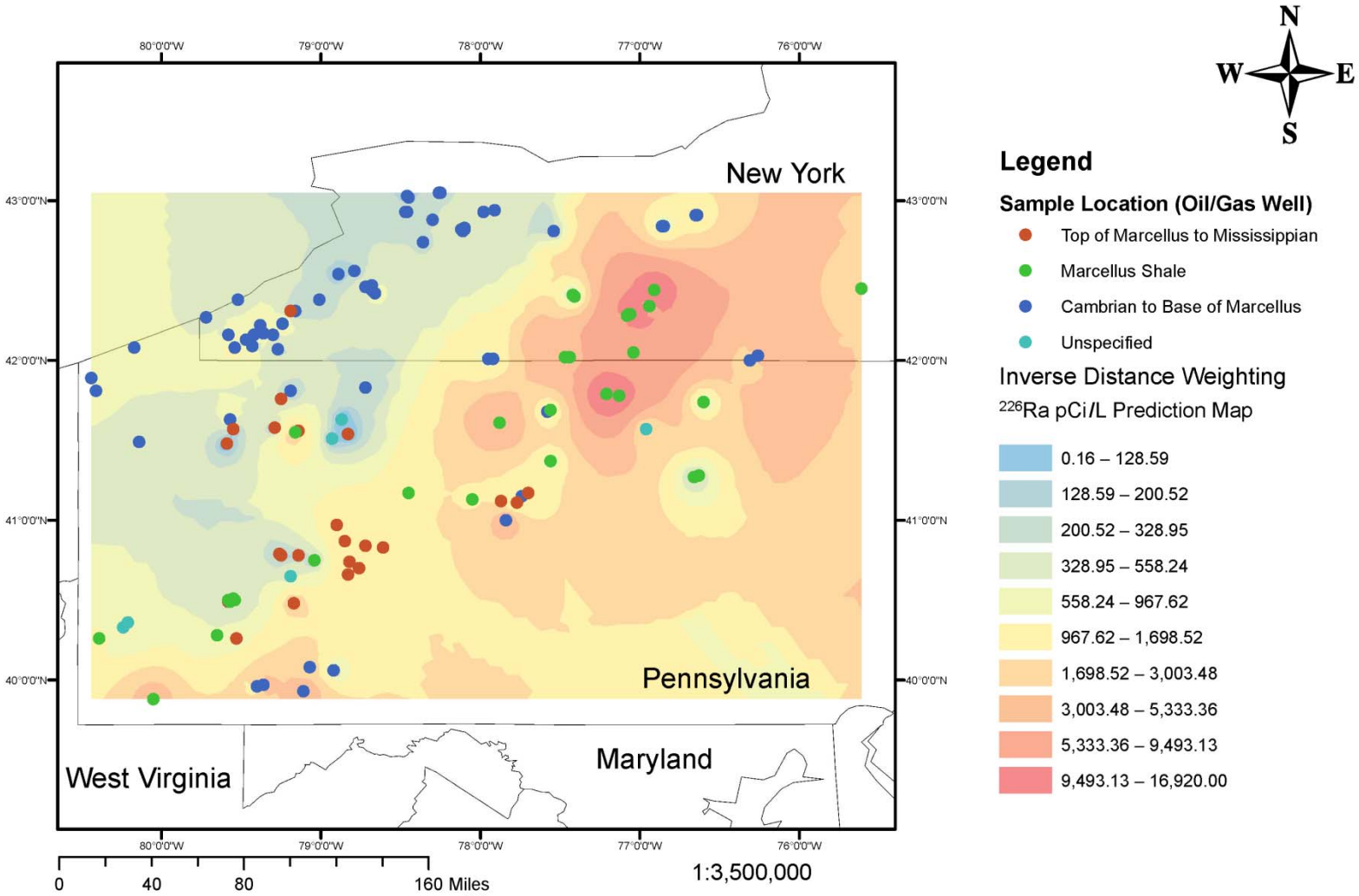

Figure 15: AppalachianBasin Oil/Gas Well ^{226}Ra pCi/L

This map displays an Inverse Distance Weighted interpolation of Appalachian Basin ^{226}Ra in oil and gas wells. Previous research measured these isotope values from the depicted sample locations (Rowan et al., 2011).

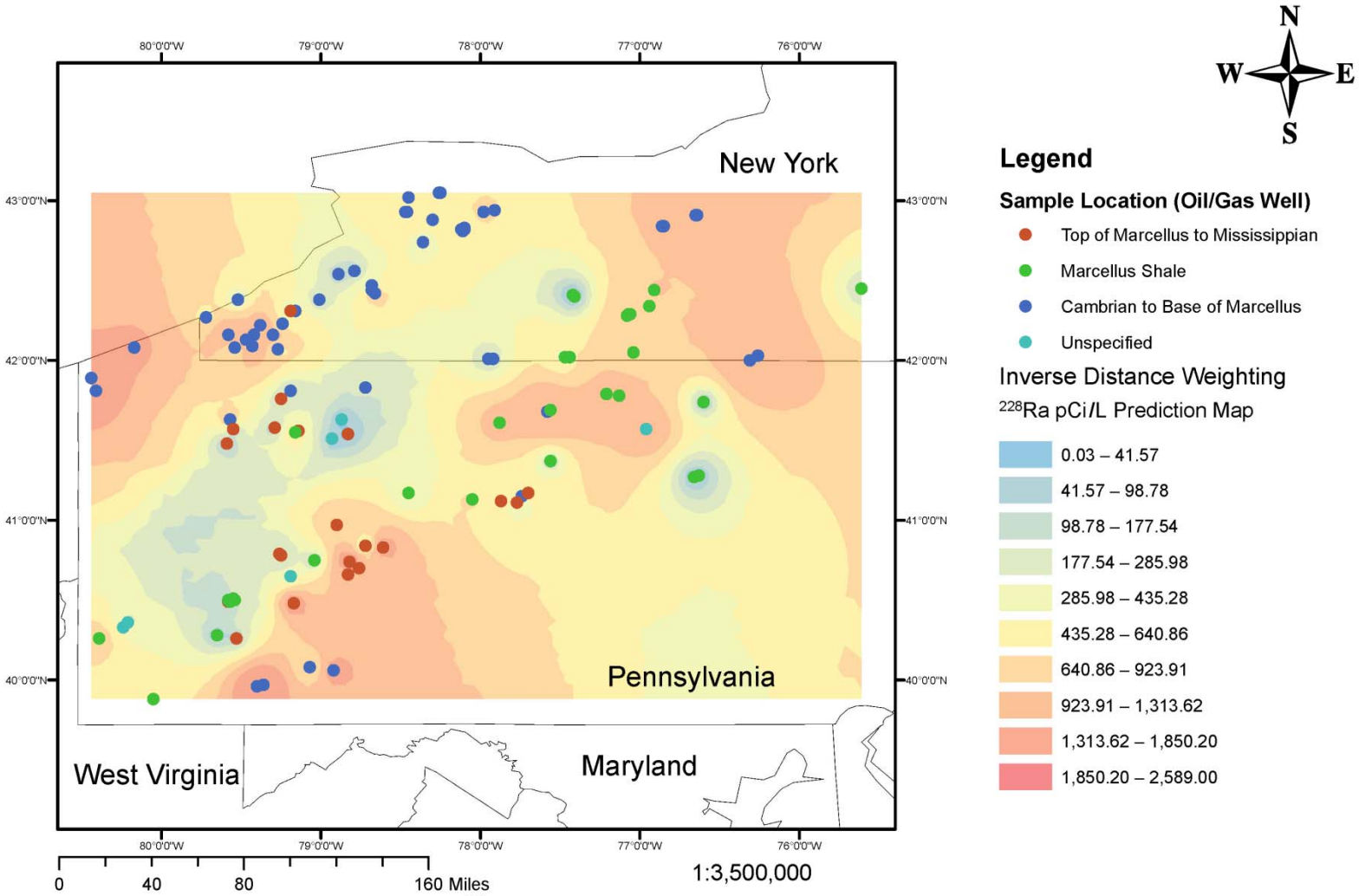

Figure 16: AppalachianBasin Oil/Gas Well ^{228}Ra pCi/L

This map displays an Inverse Distance Weighted interpolation of Appalachian Basin ^{228}Ra in oil and gas wells. Previous research measured these isotope values from the depicted sample locations (Rowan et al., 2011).

4. CONCLUSION

This study compiled 1,141 isotopic data points in the Appalachian Basin from 10 publically accessible studies. Using ESRI ArcMap, both Kriging and IDW analyses were conducted to create interpolated surfaces in an attempt to find regional trends or variations in isotopic concentrations across the Appalachian Basin. The Kriging interpolations produced the highest artifact occurrence. The difference in artifact frequency between the two methods is likely a result from how the two interpolation methods treat clustered data differently. While many of the hydrocarbon and groundwater datasets display a trend or regional variation, the data available are limited in frequency and regional extent. Artifact occurrence was frequent and there are several interpolated values far from a sampling location that will inherently have high uncertainty.

This report serves as a foundation with a hope that as future data emerge from a range of sources, the datasets can be used to reduce uncertainty and develop meaningful spatial results. The data in this report can be accessed from NETL's Energy Data eXchange (EDX) online system (https://edx.netl.doe.gov) using the following link: https://edx.netl.doe.gov/dataset/stable-isotope-data-appalachian-basin. Additional sampling locations are required to populate the dataset; however, research and modeling that incorporates subsurface geological structure and composition along with watershed data will increase the accuracy and certainty of the data. Comparing the interpolated surfaces presented in this study with historical and modern regional geologic maps could also underline the importance that surface and subsurface geology plays when interpolating in the geological sciences.

Identifying relationships in values between seemingly disparate isotopes may be one means to increase interpolation accuracy without additional datasets. Kendall and Coplen (2001) already suggest that groundwater isotopes play a large role in determining hydrogen isotope values during methanogenesis. Additional isotopic associations would facilitate interpolation research. For example, no established relationship currently links radium and carbon isotopes abundances in the Appalachian Basin; however, if a way to correlate radium and carbon isotope concentrations was found, the accuracy of the interpolated surface analyses could be expanded, which would be beneficial to hydrocarbon studies in the Appalachian Basin and worldwide.

5. REFERENCES

Baldassare, F. J.; McCaffrey, M. A.; Harper, J. A. A Geochemical Context for Stray Gas Investigations in the Northern Appalachian Basin: Implications of Analyses of Natural Gases from Neogene-through Devonian-age Strata. *The American Association of Petroleum Geologists* **2014,** *98*, 341–372.

Chanton, J.; Chaser, L.; Glasser, P.; Siegel, D. Carbon and Hydrogen Isotopic Effects in Microbial Methane from Terrestrial Environments. In *Stable Isotopes and Biosphere - Atmosphere Interactions Processes and Interactions*; Elsevier Academic Press: London, 2005; 85–105.

Coplen, T. B.; Huang, R. *Stable Hydrogen and Oxygen Isotope Ratios for Selected Sites of the National Oceanic and Atmospheric Administration's Atmospheric Integrated Research Monitoring Network (AIRMoN)*; U.S. Geological Survey Open-File Report, 2000-279; 2000.

Coplen, T. B.; Kendall, C. *Stable Hydrogen and Oxygen Isotope Ratios for Selected Sites of the U.S. Geological Survey's NASQAN and Benchmark Surface-water Networks*; U.S. Geological Survey Open-File Report, 00-160; 2000.

Etiope, G.; Drobniak, A.; Schimmelmann, A. Natural seepage of shale gas and the origin of "eternal flames" in the Northern Appalachian Basin, USA. *Marine and Petroleum Geology* **2013,** *43*, 178–186.

Faill, R. A Geologic History of the North-central Appalachians; Part 2, The Appalachian Basin from the Silurian through the Carboniferous. *American Journal of Science* **1997,** *297*, 729–761.

Friedman, I.; Redfield, A. C.; Schoen, B.; Harris, J. The Variation of the Deuterium Content of Natural Waters in the Hydrologic Cycle. *Reviews of Geophysics* **1964,** *2*, 177–224.

Islas, J. Appalachian Basin Report. *AS Energy Consulting* **2006,** 1–15.

Kendall, C.; Coplen, T. B. Distribution of oxygen-18 and deuterium in river waters across the United States. *Hydrological Processes* **2001,** *15*, 1363–1393.

Kendall, C. Resources on Isotopes. http://wwwrcamnl.wr.usgs.gov/isoig/period/c_iig.html (accessed May 15, 2014).

Molofsky, L. J.; Connor, J. A.; Wylie, A. S.; Wagner, T.; Farhat, S. K. Evaluation of Methane Sources in Groundwater in Northeastern Pennsylvania. *Groundwater* **2013,** *51*, 333–349.

Osborn, S. G.; McIntosh, J. C. Chemical and Isotopic Tracers of the Contribution of Microbial Gas in Devonian Organic-rich Shales and Reservoir Sandstones, Northern Appalachian Basin. *Applied Geochemistry* **2010,** *25*, 456–471.

Risser, D. W.; Breen, K. J. *Groundwater Quality and Simulation of Sources of Water to Wells in the Marsh Creek Valley at the U.S. Geological Survey Northern Appalachian Research Laboratory, Tioga County, Pennsylvania*; U.S. Geological Survey Scientific Investigations Report, 2012-5042; 2012.

Rowan, E. L.; Engle, M. A.; Kirby, C. S.; Kraemer, T. F. *Radium Content of Oil- and Gas-Field Produced Waters in the Northern Appalachian Basin (USA): Summary and Discussion of Data*; U.S. Geological Survey Scientific Investigations Report, 2011-5135; 2011.

Ryder. R. T. *Appalachian Basin Province*; U.S. Geological Survey Report 067; 1995.

Sharma, S.; Mulder, M. L.; Sack, A; Schroeder, K.; Hammack, R. Isotope Approach to Assess Hydrologic Connections During Marcellus Shale Drilling. *Groundwater* **2013,** *52*, 424–433.

Swezey, C. *Regional Stratigraphy and Petroleum Systems of the Appalachian Basin, North America*; U.S. Geological Survey Map I, 2768; 2002.

Jared Ciferno
Director
Strategic Center for Natural Gas and Oil
National Energy Technology Laboratory
U.S. Department of Energy

Maria Vargas
Deputy Director
Strategic Center for Natural Gas and Oil
National Energy Technology Laboratory
U.S. Department of Energy

Ray Boswell
Technology Manager
Strategic Center for Natural Gas and Oil
National Energy Technology Laboratory
U.S. Department of Energy

Elena Melchert
Program Manager
Oil and Gas Production
Office of Fossil Energy
U.S. Department of Energy

Cynthia Powell
Director
Office of Research and Development
National Energy Technology Laboratory
U.S. Department of Energy

Mark Williams
RES Program Manager
URS Corporation